Role of Te in the low-dimensional multiferroic material $FeTe_2O_5Br$

Jayita Chakraborty,[1] Nirmal Ganguli,[2] Tanusri Saha-Dasgupta,[3] and Indra Dasgupta[1,*]

[1]*Department of Solid State Physics, Indian Association for the Cultivation of Science, Jadavpur, Kolkata 700032, India*

[2]*Faculty of Science and Technology and MESA + Institute for Nanotechnology, University of Twente, P.O. Box 217, 7500 AE Enschede, The Netherlands*

[3]*S. N. Bose National Center for Basic Sciences, JD-III, Salt Lake City, Kolkata 700098, India*

(Received 28 June 2013; revised manuscript received 21 August 2013; published 9 September 2013)

Using first principles density functional calculations, we study the electronic structure of the low-dimensional multiferroic compound $FeTe_2O_5Br$ to investigate the origin of the magnetoelectric (ME) effect and the role of Te ions in this system. We find that without magnetism, even in the presence of Te 5*s* lone pairs, the system remains centrosymmetric due to the antipolar orientation of the lone pairs. Our study shows that the exchange striction within the Fe tetramers as well as between them is responsible for the ME effect in $FeTe_2O_5Br$. We also find that the Te^{4+} ions play an important role in the intertetramer exchange striction as well as contributing to the electric polarization in $FeTe_2O_5Br$, once the polarization is triggered by the magnetic ordering.

DOI: 10.1103/PhysRevB.88.094409 PACS number(s): 71.20.−b, 75.30.Et, 75.80.+q, 77.80.−e

I. INTRODUCTION

Multiferroic materials with the simultaneous presence of ferroelectricity and magnetism have been the focus of attention in recent times.[1,2] Based on the microscopic origin of ferroelectricity (FE) multiferroic materials can be classified into two different classes, namely, type-I (proper) and type-II (improper) multiferroic materials. In type-I multiferroics, ferroelectricity and magnetism stem from an independent origin and the coupling between magnetism and ferroelectricity is usually weak. In these materials, ferroelectricity typically appears at higher temperatures than magnetism, and the magnitude of spontaneous electric polarization (*P*) is often large (∼10–100 $\mu C/cm^2$). One possible mechanism for ferroelectricity in a type-I multiferroic material is lone-pair driven. It is well known that cations containing highly polarizable 5*s* or 6*s* lone pairs of valence electrons have a strong tendency to break the local inversion symmetry of the crystal. This lone-pair driven mechanism was identified as the source of ferroelectric instability in $BiFeO_3$.[3] In contrast, type-II multiferroics, where ferroelectricity may arise due to a particular kind of magnetic ordering that breaks the inversion symmetry, are more interesting from an application point of view due to the strong coupling between magnetism and FE.[4,5] However, the magnitude of electric polarization in these materials is usually very small ($\sim 10^{-2}$ $\mu C/cm^2$). For type-II multiferroics, nonsymmetric lattice distortion and ferroelectric order may be induced through exchange striction,[6,7] a spin current mechanism,[8] or inverse Dzyaloshinskii-Moriya (DM) interactions.[9] In particular, the exchange striction is considered to induce ferroelectricity in some collinear antiferromagnets such as $HoMnO_3$ (Ref. 6) and Ca_3CoMnO_6.[7,10,11] While strong coupling between the magnetic and ferroelectric order parameters makes them attractive, their real applications have been restricted by the small magnitude of the polarization values. A possible way to overcome this difficulty could be to combine the best features of type-I and type-II multiferroics. In this context, the transition metal (TM) selenium (Se) and tellurium (Te) oxihalides may offer an attractive possibility as they exhibit exotic magnetic properties driven by the geometric frustration in low dimensions and they also contain a stereochemically active lone pair in Te^{4+} and Se^{4+} that may result in lone-pair driven ferroelectricity as in the case of type-I mutiferroics. Interestingly, some of these systems exhibit multiferroic behavior. An example of such a system is $FeTe_2O_5Br$. It adopts a layered structure, where individual layers consist of geometrically frustrated iron tetramer units $[Fe_4O_{16}]$ linked by the $[Te_4O_{10}Br_2]^{6-}$ groups.[12] However, the structure remains centrosymmetric even in the presence of Te-$5s^2$ lone pairs. The high-temperature fit to the susceptibility data shows a negative Curie-Weiss temperature ($\theta_{CW} = -98$ K), indicating strong antiferromagnetic interactions between the $Fe^{3+}(d^5)$ ions.[12] The system develops long range magnetic order at a considerably low temperature $T_{N_1} = 11$ K, followed by a second magnetic transition at $T_{N_2} = 10.5$ K.[13] The first transition at T_{N_1} is a paramagnetic to a high-temperature incommensurate magnetic state (HT-IC) with a constant wave vector $q_{IC1} = (0.5,0.466,0.0)$ and is immediately followed by another transition at $T_{N_2} = 10.5$ K into the low-temperature incommensurate (LT-IC) multiferroic state. The amplitude modulated magnetic order in the LT-IC phase is described with the wave vector $q = (0.5,0.463,0)$ and concomitantly with the magnetic order a ferroelectric polarization ($P = 8$ $\mu C/m^2$) is induced perpendicular to q and the direction of the Fe^{3+} moments.[14] As the polarization is found to be triggered by magnetic ordering, the resulting small value of the polarization provides direct evidence that $FeTe_2O_5Br$ is an example of a type-II (improper) multiferroic, contrary to the original expectation of combining the features of type-I and type-II multiferroics. A recent study[15] on the magnetic ordering in the HT-IC phase of $FeTe_2O_5Br$ showed that while the inversion symmetry is already broken in the HT-IC phase, the ferroelectricity is only realized in the LT-IC phase. The difference in the orientation of the magnetic moments and phase shift of the amplitude modulated waves between the two magnetic structures is suggested to be responsible for the realization of ferroelectricity in the LT-IC phase. In addition, there is evidence of minute displacements of the Te^{4+} ions in the LT-IC phase, and these subtle displacements may be important for the electric polarization in this phase.[15] In view of the above, it is suggested that polarization is possibly driven

by exchange striction on the interchain bond containing highly polarizable Te lone-pair electrons. In the search for a suitable spin Hamiltonian, magnetic susceptibility was analyzed by various groups. An early report suggested that magnetic susceptibility can be explained by considering the dominant interactions within the Fe tetramers.[12] A recent study, however, shows that the system should be described as a system of alternating antiferromagnetic $S = 5/2$ chains with strong Fe-O-Te-O-Fe bridges weakly coupled by two-dimensional frustrated interactions.[16]

The preceding discussion suggests that it will be important to clarify the role of Te ions in the multiferroic property of $FeTe_2O_5Br$. In particular, it will be interesting to understand the interplay of magnetic interaction and the activity of the Te^{4+} lone pairs and eventually their combined role in the ferroelectric polarization. In the present paper we have examined this issue in detail using *ab initio* electronic structure calculations. The remainder of the paper is organized as follows. In Sec. II we describe the crystal structure along with the computational details. Section III is devoted to a detailed discussion of our results on the electronic structure calculations. Finally, a summary and conclusions are given in Sec. IV.

II. CRYSTAL STRUCTURE AND COMPUTATIONAL DETAILS

$FeTe_2O_5Br$ crystallizes in the monoclinic space group $P21/c$. The crystallographic unit cell has an inversion center. The lattice parameters for $FeTe_2O_5Br$ are $a = 13.396$ Å, $b = 6.597$ Å, $c = 14.289$ Å, and $\beta = 108.12^\circ$.[12] The unit cell (depicted in Fig. 1) contains 72 atoms.

There are two crystallographically inequivalent Fe^{3+} ions in the structure which are in a distorted $[FeO_6]$ octahedral environment. Four such octahedra share their edges with each other and form a $[Fe_4O_{16}]$ iron tetramer cluster (see the inset of Fig. 1). These iron tetramers are linked by $[Te_4O_{10}Br_2]^{6-}$ units forming a layered structure in the bc plane. The layers are weakly connected via van der Waals forces as they stack along the monoclinic a axis.

The first principles density functional theory (DFT) calculations have been performed using the plane-wave based projector augmented wave (PAW)[17] method as implemented in the Vienna *ab initio* simulation package (VASP).[18] We have used a local density approximation (LDA) to the exchange correlation functional. The localized Fe-d states were treated in the framework of local spin-density approximation (LSDA) + U method,[19] where calculations were done for several values of $U_{\text{eff}} = U - J$ in the range 0 (LDA)–5 eV. The calculations for the unit cell were performed with a $(4 \times 8 \times 4)$ Γ centered k point mesh and 550 eV as the plane-wave cutoff energy. In order to simulate the magnetic structure we have neglected the amplitude modulation and have approximated the incommensurate wave vector $q \sim (0.5,0.463,0)$ by a commensurate one (0.5,0.5,0), and have generated a supercell $(2 \times 2 \times 1)$ of the original unit cell containing 288 atoms. For the calculations with the supercell, a plane-wave cutoff energy of 500 eV was used along with a $(1 \times 2 \times 2)$ Γ centered k point mesh. All structural relaxations were carried out until the Hellman-Feynman forces became less than 0.01 eV/Å.

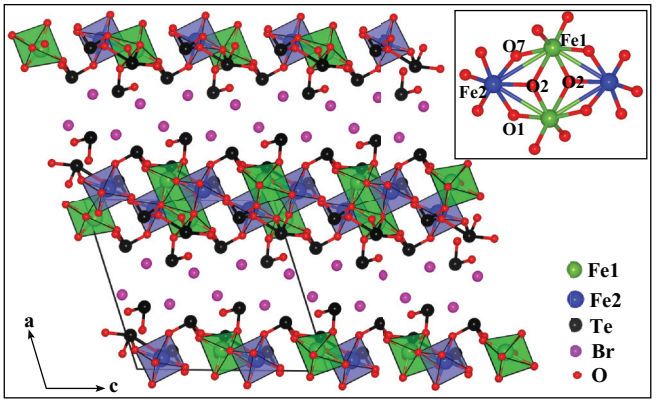

FIG. 1. (Color online) Layered structure of $FeTe_2O_5Br$. The inset shows one tetramer unit.

For the derivation of the low energy model Hamiltonian and identification of various exchange paths we have employed the Nth order muffin-tin orbital (NMTO) downfolding method.[20,21] The NMTO downfolding method is an efficient *ab initio* scheme to construct a low energy, few band, tight-binding model Hamiltonian. The low energy model Hamiltonian is constructed by the energy selective downfolding method, where high energy degrees of freedom are integrated out from the all orbital LDA calculations. The Fourier transform of the resulting low energy Hamiltonian yields the effective hopping parameters which can be utilized to identify the dominant exchange paths.

III. RESULTS AND DISCUSSIONS

A. Non-spin-polarized calculation

To begin with, we have investigated the electronic structure of $FeTe_2O_5Br$ without magnetic order. The non-spin-polarized total and partial density of states are shown in Fig. 2. The density of states (DOS) is consistent with the $Fe^{3+}Te_2^{4+}O_5^{2-}Br^{1-}$ nominal ionic formula for the system. Figure 2 reveals that O-p and Br-p states are completely occupied while the Fermi level (E_F) is dominated by the Fe-d states. The occupied Te-5s states lie far below the E_F. The empty Te-5p states lie above the Fermi level, spreading on an energy range 2–6 eV with respect to the Fermi level. There is a significant admixture of Te-5s and Te-5p states with the O-p states, which suggests the hybridization between Te and O, which in turn hybridizes with Fe-d states crossing the Fermi level (see the insets in Fig. 2).

The presence of Te in a 4+ oxidation state suggests the possibility of the stereochemical activity of a Te lone pair formed from $5s^2$ electrons. In order to visualize the lone pairs arising from $5s^2$ electrons of Te^{4+} ions, we have calculated the electron localization function (ELF).[22,23] The ELF is defined as follows:

$$\text{ELF} = \left[1 + \left(\frac{D}{D_h}\right)^2\right]^{-1}, \tag{1}$$

where

$$D = \frac{1}{2}\sum_i |\nabla\phi_i|^2 - \frac{1}{8}\frac{|\nabla\rho|^2}{\rho}$$

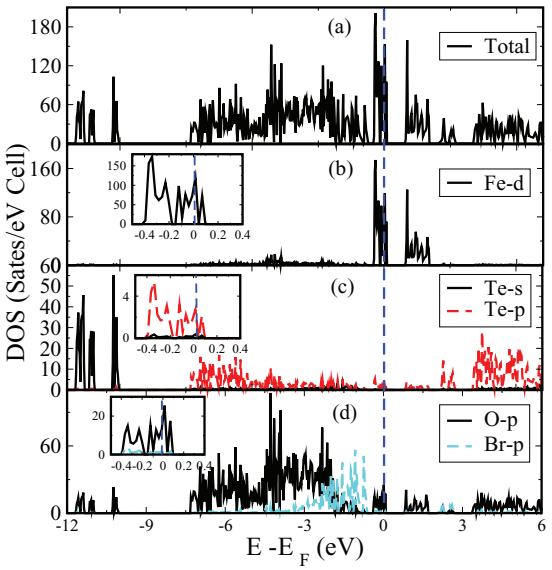

FIG. 2. (Color online) The non-spin-polarized density of states for $FeTe_2O_5Br$. (a) The total DOS, orbital-projected density of states for (b) Fe-d, (c) Te-s and Te-p, and (d) O-p and Br-p. The insets show the orbital characters near the Fermi level.

and

$$D_h = \frac{3}{10}(3\pi^2)^{5/3}\rho^{5/3}.$$

ρ is the electron density and ϕ_i are the Kohn-Sham wave functions. The ELF is defined in such a way that its value lies between 0 and 1. The values are close to 1 when, in the vicinity of one electron, no other electron with the same spin may be found. For instance, this would occur in bonding pairs or *lone pairs*.[24] From the plot of the electron localization function, in the experimental centrosymmetric structure[12] displayed in Fig. 3, we find that the electron density around Te is asymmetric and forms a usual lobe shape arising from the 5s lone pair of Te. It has been pointed out by Watson and Parker that the hybridization with anion p orbitals (oxygen 2p) plays an important role in the formation of an asymmetric

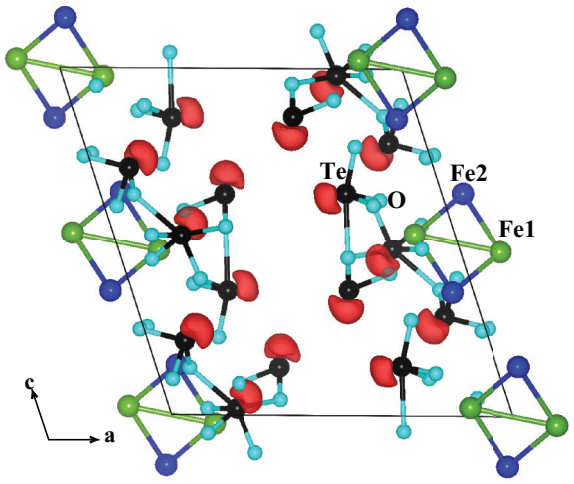

FIG. 3. (Color online) Electron localization function within a unit cell. The isosurfaces are visualized for a value of 0.9.

lobe shaped isosurface of the electron localization function for sterically active lone pairs.[25] We gather from the DOS shown in Fig. 2 that the occupied Te s and O p orbitals hybridize to form a pair of occupied bonding and antibonding states. This Te-5s–O-2p mixed state further hybridizes with empty Te-5p states. As a consequence both the Te-5s and Te-5p states are involved in the formation of the asymmetric electron distribution where empty Te-5p orbitals are able to interact due to the presence of Te-s–O-p occupied antibonding states. This emphasizes the importance of the O-p states in the formation of lone pairs.

In order to quantify the hybridization, we have calculated the hybridization index defined as follows:

$$H_{I-l,J-l'} = \sum_k \left(\sum_i h^{i,k}_{I-l,J-l'} \right) \times \text{weight}(k),$$

where

$$h^{i,k}_{I-l,J-l'} = \sum_{I,J,m,m'} w^{(I)}_{lm,i,k} w^{(J)}_{l'm',i,k};$$

$w^{(I)}_{lm,i,k}$ are the coefficients in the spherical harmonic decomposition of the local (partial) charge, associated with the ith Kohn-Sham orbital,[26] around the Ith atom. l,m indicates the orbital and the magnetic quantum numbers, respectively, I and J are atom indices, $I \in$ {Te atoms} and $J \in$ {O atoms}, and i and k stand for the band index and k points, respectively. Weight(k) is the weight on each k point in the irreducible Brillouin zone that is necessary for the integration. Our calculations find that the hybridization index between Te-p and O-p is 6.13 and that between Te-s and O-p it is 3.80 for the experimental centrosymmetric structure,[12] indicating a sizable hybridization between Te and O. It is interesting to note that these lone pairs, however, do not promote structural distortion and the structure remains centrosymmetric, as the pair of lobes are arranged in an opposite manner, resulting in canceling polarization of the structure, as is evident from Fig. 3.

B. Spin-polarized calculation

We next consider magnetism and its impact on the crystal structure and ferroelectric polarization. In order to simulate the low-temperature magnetic order found in the LT-IC phase, we have made a (2 × 2 × 1) supercell which contains 288 atoms. As mentioned before, in our calculation we have neglected the amplitude modulation. We consider various antiferromagnetic (AFM) configurations (see Fig. 4), depending on the arrangement of Fe spins within each tetramer as well as between the neighboring tetramers. In the AFM1 configuration, not only are Fe1 spins aligned antiparallel to Fe2 within each tetramer [see the inset of Fig. 4(a)], but also each tetramer is antiferromagnetically coupled along the a and b directions, leading to q = (0.5,0.5,0). The AFM2 configuration differs from the AFM1 configuration only in the arrangement of spins within each tetramer [see the inset of Fig. 4(b)], where a pair of Fe1 spins in a tetramer are antiparallel and the same is true for a pair of Fe2 spins. Finally, in the AFM3 configuration, the arrangement of Fe1 and Fe2 spins in each tetramer is identical to AFM1 but the tetramers are coupled ferromagnetically along the a, b, and c directions, leading to q = (0,0,0). The

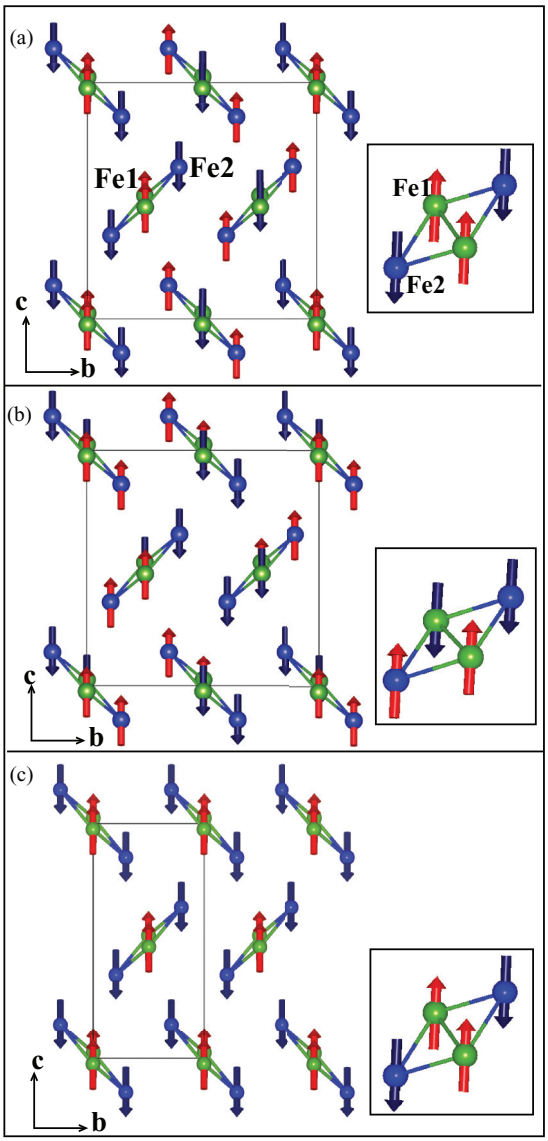

FIG. 4. (Color online) Various antiferromagnetic configurations: (a) AFM1, (b) AFM2, and (c) AFM3.

results of our calculations are displayed in Table I. The results reveal that among the magnetic configurations considered here, AFM1 has the lowest energy. All magnetic states are found to be insulating and the magnetic moment at the Fe site is $m_{\mathrm{Fe}} \sim 4.2\mu_B$. The rest of the moments are at the oxygen ($m_{\mathrm{O}} \sim 0.13\mu_B$) and bromine ($m_{\mathrm{Br}} \sim 0.09\mu_B$) sites, arising due to the Fe-O and Fe-Br hybridization effect.

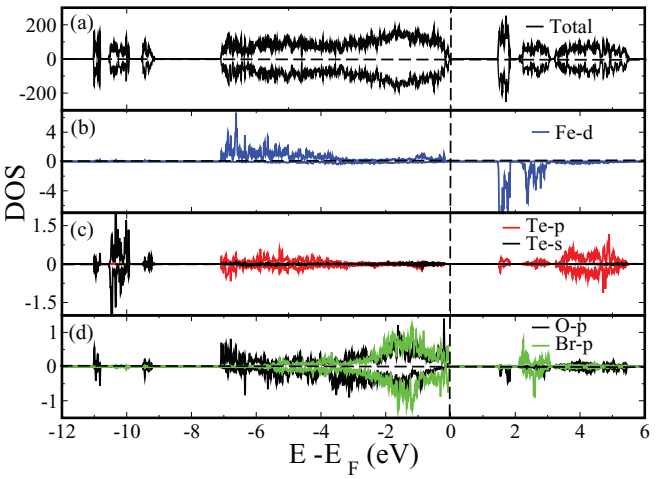

FIG. 5. (Color online) The density of states for $FeTe_2O_5Br$ in the AFM1 configuration with an experimental structure. (a) Total DOS (states/eV cell). Orbital projected DOS (states/eV atom) for (b) Fe-d, (c) Te-s and Te-p, and (d) O-p and Br-p states.

The total density of states as well as its projection onto different atomic orbitals for the AFM1 phase are shown Figs. 5(a)–5(d). Focusing on Fig. 5(b), we find that Fe-d states in the majority spin channel are completely occupied while the minority states are completely empty, which is consistent with the Fe^{3+} valence state of Fe with a $3d^5$ configuration. Such a half filled configuration promotes the AFM order.

Next, we have identified the dominant exchange paths and the relevant spin Hamiltonian using the Nth order muffin-tin orbital (NMTO) downfolding method.[20,21] In order to derive a low energy effective model Hamiltonian, we have retained the isolated Fe band complex near the Fermi level for a non-spin-polarized calculation and downfolded the rest with the choice of two energy points E_0 and E_1. The downfolded bands in comparison to the all orbital LDA band structure is shown in Fig. 6, and we note that the agreement is very good. The Fourier transform of the low energy Hamiltonian $H_k \rightarrow H_R$ [where H_R is given by $H_R = \sum_{ij} t_{ij}(c_i^\dagger c_j + \mathrm{H.c.})$] gives the effective hopping parameters between the various Fe atoms. The various hopping integrals can be utilized to identify the dominant exchange paths. For strongly correlated systems, the antiferromagnetic contribution to the exchange integral can be computed using $J^{\mathrm{AFM}} = 4\frac{\sum_{i,j} t_{ij}^2}{\bar{U}}$, where $\bar{U}$ is the effective on-site Coulomb interaction and t_{ij} corresponds to the hopping via superexchange paths. The ratio of the various exchange interactions are displayed in Table II and

TABLE I. The relative energies, magnetic moments, and band gaps for different magnetic configurations are listed here.

	$U_{\mathrm{eff}} = 3$ eV				$U_{\mathrm{eff}} = 5$ eV			
Magnetic config.	ΔE (meV)	Band gap (eV)	m_{Fe1} (μ_B)	m_{Fe2} (μ_B)	ΔE (meV)	Band gap (eV)	m_{Fe1} (μ_B)	m_{Fe2} (μ_B)
FM	49.7	1.3	4.1	4.1	34.1	1.5	4.2	4.2
AFM1	0.0	1.2	4.1	4.1	0.0	1.6	4.2	4.2
AFM2	15.7	1.4	4.1	4.1	10.1	1.6	4.2	4.2
AFM3	9.0	1.5	4.1	4.1	5.8	1.7	4.2	4.2

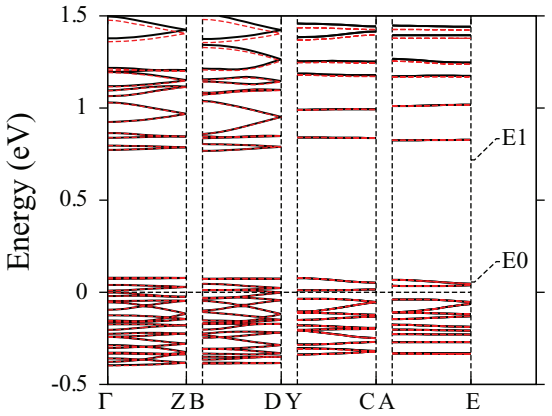

FIG. 6. (Color online) Downfolded band structure (red dotted line) compared with a full orbital LDA band structure (black solid line) of $FeTe_2O_5Br$.

the various exchange paths are indicated in Fig. 7. In last two columns we have also reproduced the ratio of exchange interactions obtained in Ref. 16 using the total energy method. In Ref. 16, it is reported that the alternating spin chain model is more appropriate instead of the tetramer model suggested for this system as the intertetramer superexchange (J_4) mediated by Fe-O-Te-O-Fe bridges is appreciable. The values of the exchange interactions obtained from the NMTO downfolding method reveal that, in addition to the intracluster exchange interactions J_1, J_2, J_3, the intercluster exchange interaction J_4 is substantial, supporting the suggestion made in Ref. 16. However, the quantitative values of the exchange interactions, specifically the values of $\frac{J_1}{J_2}$ and $\frac{J_4}{J_2}$, differ in the two studies, possibly due to the different calculation schemes adopted in these two independent investigations.

We next investigated the impact of magnetism on crystal structure, viz., exchange striction. We have carried out the structure optimization with nonmagnetic, ferromagnetic, and AFM1 magnetic configurations. In this optimization, the cell parameters were fixed to the experimental values, but the positions of the atoms were allowed to relax. The change in bond lengths with respect to the unrelaxed (experimental) structure corresponding to various exchange paths are displayed in

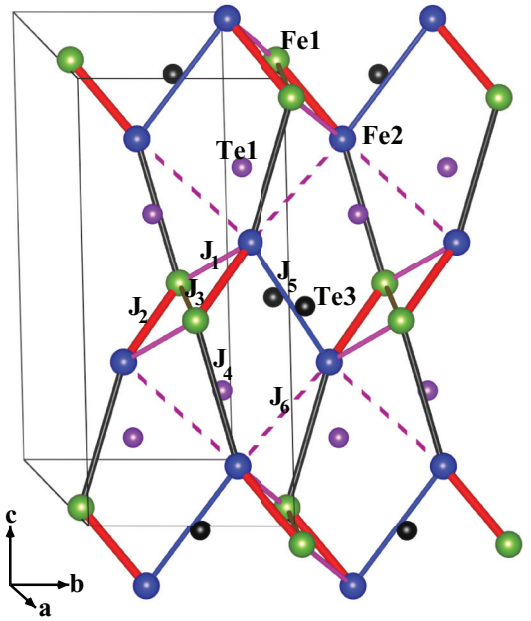

FIG. 7. (Color online) Structure of $FeTe_2O_5Br$; exchange paths are indicated.

Table III for the AFM1, FM, and non-spin-polarized cases. The bond lengths hardly change due to the ionic relaxations for nonmagnetic and ferromagnetic cases, indicating negligible exchange striction. The maximum change in ionic positions occurs in the relaxed structure with AFM1 magnetic ordering. The dominant changes correspond to the exchange path J_3 involving oxygens and J_5 involving the Te ions (marked in bold in Table III). Our calculations provide a direct evidence that the exchange paths J_3 and J_5 are responsible for the spin-phonon coupling in this compound. The importance of the exchange path J_5 was also anticipated in Ref. 16.

To obtain an estimate of the impact of structural distortion on the lone pairs, we computed the hybridization index for the relaxed structure in the AFM1 phase. The H indices for the relaxed structure are found to be 17.305 and 11.015 between Te-p and O-p, and Te-s and O-p, respectively, as opposed to 17.00 and 10.99 in the AFM1 phase for the

TABLE II. Exchange interactions along different exchange paths obtained from the NMTO downfolding method and energy method (Ref. 16) have been tabulated here.

Exchange	Distance (Å)	Exchange paths, bond lengths, and angles	J_i/J_2 from NMTO ($U_{\text{eff}} = 3$ eV)	J_i/J_2 in Ref. 16 ($U_{\text{eff}} = 3$ eV)	J_i/J_2 in Ref. 16 ($U_{\text{eff}} = 4$ eV)
J_1	3.16	∠Fe1-O1-Fe2 = 101.8° ∠Fe1-O2-Fe2 = 99.5°	0.89	0.46	0.35
J_2	3.34	∠Fe1-O7-Fe2 = 110.2° ∠Fe1-O2-Fe2 = 95.79°	1	1	1
J_3	3.43	∠Fe1-O2-Fe1 = 101.7°	0.44	0.33	0.34
J_4	4.76	Fe1-O-Te1-O-Fe2 Fe1-O-Te4-O-Fe2	0.26	0.62	0.59
J_5	4.77	Fe2-O-Te3-O-Fe2	0.05	0.04	0.0
J_6	5.10	Fe1-O-Te1-O-Fe1	0.15	0.27	0.26
J_7	5.52	O-O ∼ 2.81	0.02		

TABLE III. The bond lengths between the Fe atoms in the experimental structure and the change in the Fe-Fe bond lengths upon relaxation within different magnetic configurations have been listed here. +(−) signs indicate the increment (decrement) of the distance.

Exchange paths	Bond length (Å) expt. structure	Change in the bond length upon relaxation (Å) with respect to the experimental structure		
		AFM1	FM	NM
J_1 (Fe1-Fe2)	3.16	−0.04	−0.01	−0.01
J_2 (Fe1-Fe2)	3.34	−0.03	0.00	0.00
J_3 (Fe1-Fe1)	**3.43**	**−0.11**	**−0.04**	**−0.02**
J_4 (Fe1-Fe2)	4.76	0.02	0.00	0.00
J_5 (Fe2-Fe2)	**4.77**	**0.05**	**0.02**	**0.01**
J_6 (Fe2-Fe2)	5.10	0.00	0.00	0.00

centrosymmetric experimental structure.[12] This indicates that the Te-O hybridization increases as a result of the structural distortion, pointing to the importance of Te lone pairs. Finally, to access the asymmetry between two neighboring lobe shaped charge distributions of the lone pairs, we have calculated the moment of the electron localization function ($\vec{M}^i_{\rm ELF}$) for the ith Te atom as follows:

$$\vec{M}^i_{\rm ELF} = \int_{|\vec{r}|=0}^{R} d^3r \, {\rm ELF}(\vec{r})\vec{r}, \qquad (2)$$

where $\vec{r}$ is the position vector assuming the ith Te atom at the origin and R is a suitably chosen radius of a sphere that covers the range of ELF around the ith Te atom. We find that the sum of $\vec{M}^i_{\rm ELF}$'s vanishes for a pair of suitably chosen Te atoms in the centrosymmetric experimental structure,[12] whereas it has a finite value for the same pairs of atoms in the relaxed structure. This observation suggests that, unlike the centrosymmetric experimental structure where the local dipole moments cancel pairwise, leading to no net polarization, in the relaxed magnetic structure they do not cancel out. (The average ELF moment for a pair of Te atoms in a relaxed magnetic structure is 7.2 Å.) This calculation hints at the activation of the stereochemical activity of the Te ions once the polarization is triggered by the magnetic ordering, as elaborated in the next section. In fact, the minute displacements of the Te^{4+} ions below T_{N_2} in the multiferroic LT-IC phase has been corroborated by the nuclear quadrupolar resonance (NQR) results.[15]

C. Polarization

We have calculated the ferroelectric polarization using the Berry phase method[27] as implemented in the Vienna *ab initio* simulation package (VASP).[28] The polarization calculations are carried out with the idealized magnetic configuration AFM1 for several $U_{\rm eff}$ values. Our results are summarized in Table IV. The direction of polarization is the same with different $U_{\rm eff}$ values, but the magnitude decreases with the increasing value of $U_{\rm eff}$. The calculated polarization for $FeTe_2O_5Br$ is large compared to the experimental value. Such an overestimation is also reported for other systems,[29,30] and may be attributed to the idealized magnetic structure considered in our calculation. In view of the fact that upon ionic relaxation the bond lengths corresponding to the exchange path J_3 and J_5 change substantially, we have investigated the impact of the change in bond length on the exchange interaction and hence on the values of the polarization.

The exchange interaction J_3 involves Fe-O-Fe, the superexchange pathway, and therefore obeys the Anderson-Goodenough-Kanamori rules. When the Fe-Fe distance in the J_3 exchange path is reduced, not only does the J_3 increase, but the value of the polarization also increases, indicating the importance of this superexchange path on polarization. High resolution synchrotron x-ray diffraction, however, did not detect significant structural changes for this bond.[16] Next we have investigated the J_5 exchange path involving the Te ions. In Ref. 16, it is reported that the only sizable change in the LT-IC phase corresponds to the shortening of the Fe2-Te3 distance in the J_5 exchange pathway. In order to see how the displacement of Te3 ions affects the exchange interaction J_5 and in turn its effect on the electric polarization, we have changed the distance between Fe2-Te3 (d_1) (also the distance d_2 between Fe2-Te3) (see the inset of Fig. 8) and computed the exchange interaction J_5 and the ferroelectic polarization. In Fig. 8, we have plotted the polarization as a function of the change in exchange interaction ΔJ_5 (between the distorted and the experimental structure). ΔJ_5 may be considered as a measure of the spin-phonon interaction mediated by the Te ions. Polarization increases as ΔJ_5 is increased, and this polarization originates from the spin-phonon coupling corresponding to the J_5 exchange pathway. Our calculations reveal that polarizable lone pairs enhance the spin-phonon coupling upon exchange striction in the AFM1 phase, which in turn leads to ferroelectric polarization. In order to check the role of Te ions in the polarization, we have carried out a constrained ionic relaxation calculation in which the positions of the Te ions were kept fixed and other ionic positions were

TABLE IV. Calculated electric polarizations with an AFM1 magnetic configuration with different values of the Coulomb interaction parameter U for the relaxed structure are listed here.

$U_{\rm eff}$ values (eV)	Polarization (μC/m^2)
1	217.7
2	208.0
3	198.0
4	187.8
5	177.7

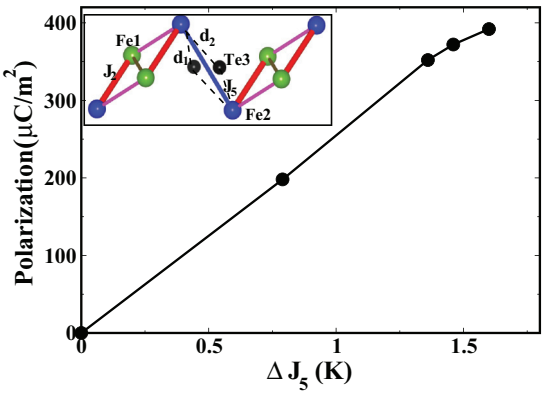

FIG. 8. (Color online) Variation of polarization with ΔJ_5. The inset shows the J_5 exchange path involving Te3 ions.

allowed to relax for the AFM1 configuration with $U_{\text{eff}} = 4$ eV. The value of polarization is calculated to be 102 μC/m^2, substantially reduced from the polarization (187.8 μC/m^2) calculated for the relaxed structure where the Te ions are also moved from their centrosymmetric positions. This result suggests that exchange striction within the Fe tetramers, as well as between them mediated by Te ions, are responsible for the magnetoelectric (ME) effect in $FeTe_2O_5Br$. Interestingly, the magnetic ordering also triggers the stereochemical activity of Te ions, giving rise to a feedback mechanism.

IV. CONCLUSIONS

We have investigated the electronic properties of a multiferroic compound $FeTe_2O_5Br$ by using density functional theory to elucidate the role of Te ions on the ferroelectric polarization of this system. We find that, in the absence of magnetism, the system remains centrosymmetric due to the antipolar orientation of the Te lone pairs that does not promote structural distortion. The results from our calculations reveal that $FeTe_2O_5Br$ is an improper multiferroic where exchange striction within the Fe tetramers as well as between them is responsible for the magnetoelectric (ME) effect. We find that the electric polarization is very sensitive to the J_5 exchange path involving the polarizable Te^{4+} lone pairs. Te-5*s* lone pairs show stereochemical activity only when the polarization is triggered by the magnetic ordering.

ACKNOWLEDGMENTS

I.D. thanks the Department of Science and Technology, Government of India for financial support, and J.C. thanks CSIR, India [Grant No. 09/080(0615)/2008-EMR-1] for funding through a research fellowship.

*sspid@iacs.res.in

[1] T. Kimura, T. Goto, H. Shintani, K. Ishizaka, T. Arima, and Y. Tokura, Nature (London) **426**, 55 (2003).
[2] N. A. Spaldin and M. Fiebig, Science **309**, 391 (2005).
[3] P. Ravindran, R. Vidya, A. Kjekshus, H. Fjellvag, and O. Eriksson, Phys. Rev. B **74**, 224412 (2006).
[4] D. I. Khomskii, J. Magn. Magn. Mater. **306**, 1 (2006).
[5] S. W. Cheong and M. Mostovoy, Nat. Mater. **6**, 13 (2007).
[6] N. Lee, Y. J. Choi, M. Ramazanoglu, W. Ratcliff, V. Kiryukhin, and S.-W. Cheong, Phys. Rev. B **84**, 020101 (2011).
[7] Y. J. Choi, H. T. Yi, S. Lee, Q. Huang, V. Kiryukhin, and S.-W. Cheong, Phys. Rev. Lett. **100**, 047601 (2008).
[8] H. Katsura, N. Nagaosa, and A. V. Balatsky, Phys. Rev. Lett. **95**, 057205 (2005).
[9] I. A. Sergienko and E. Dagotto, Phys. Rev. B **73**, 094434 (2006).
[10] H. Wu, T. Burnus, Z. Hu, C. Martin, A. Maignan, J. C. Cezar, A. Tanaka, N. B. Brookes, D. I. Khomskii, and L. H. Tjeng, Phys. Rev. Lett. **102**, 026404 (2009).
[11] Y. Zhang, H. J. Xiang, and M. H. Whangbo, Phys. Rev. B **79**, 054432 (2009).
[12] R. Becker, M. Johnsson, R. K. Kremer, H.-H. Klauss, and P. Lemmens, J. Am. Chem. Soc. **128**, 15469 (2006).
[13] M. Pregelj, A. Zorko, O. Zaharko, Z. Kutnjak, M. Jagodič, Z. Jagličić, H. Berger, M. de Souza, C. Balz, M. Lang *et al.*, Phys. Rev. B **82**, 144438 (2010).
[14] M. Pregelj, O. Zaharko, A. Zorko, Z. Kutnjak, P. Jeglič, P. J. Brown, M. Jagodič, Z. Jagličić, H. Berger, and D. Arčon, Phys. Rev. Lett. **103**, 147202 (2009).
[15] M. Pregelj, P. Jeglič, A. Zorko, O. Zaharko, T. Apih, A. Gradisek, M. Komelj, H. Berger, and D. Arčon, Phys. Rev. B **87**, 144408 (2013).
[16] M. Pregelj, H. Jeschke, H. Feldner, R. Valentí, A. Honecker, T. Saha-Dasgupta, H. Das, S. Yoshii, T. Morioka, H. Nojiri *et al.*, Phys. Rev. B **86**, 054402 (2012).
[17] P. E. Blöchl, Phys. Rev. B **50**, 17953 (1994).
[18] G. Kresse and J. Furthmüller, Phys. Rev. B **54**, 11169 (1996).
[19] S. L. Dudarev, G. A. Botton, S. Y. Savrasov, C. J. Humphreys, and A. P. Sutton, Phys. Rev. B **57**, 1505 (1998).
[20] O. K. Andersen and T. Saha-Dasgupta, Phys. Rev. B **62**, R16219 (2000).
[21] O. K. Andersen, T. Saha-Dasgupta, R. W. Tank, C. Arcangeli, O. Jepsen, and G. Krier, in *Electronic Structure and Physical Properties of Solids, The Uses of the LMTO Method*, edited by H. Dreysse, Springer Lecture Notes in Physics, Vol. 535 (Springer, Berlin, 2000), pp. 3–84.
[22] B. Silvi and A. Savin, Nature (London) **371**, 683 (1994).
[23] A. Savin, R. Nesper, S. Wengert, and T. F. Fässler, Angew. Chem., Int. Ed. Engl. **36**, 1808 (1997).
[24] A. Savin, O. Jepsen, J. Flad, O. K. Andersen, H. Preuss, and H. G. von Schnering, Angew. Chem., Int. Ed. Engl. **31**, 187 (1992).
[25] G. W. Watson, S. C. Parker, and G. Kresse, Phys. Rev. B **59**, 8481 (1999).
[26] H. Häkkinen, M. Moseler, and U. Landman, Phys. Rev. Lett. **89**, 033401 (2002).
[27] R. D. King-Smith and D. Vanderbilt, Phys. Rev. B **47**, 1651 (1993); R. Resta, Rev. Mod. Phys. **66**, 899 (1994).
[28] G. Kresse and J. Hafner, Phys. Rev. B **47**, 558 (1993).
[29] E. J. Kan, H. Xiang, Y. Zhang, C. Lee, and M.-H. Whangbo, Phys. Rev. B **80**, 104417 (2009).
[30] H. J. Xiang and M.-H. Whangbo, Phys. Rev. Lett. **98**, 246403 (2007).